

Electron attachment to POCl_3 : Measurement and theoretical analysis of rate constants and branching ratios as a function of gas pressure and temperature, electron temperature, and electron energy

Jane M. Van Doren

Department of Chemistry, Holy Cross College, Worcester, Massachusetts 01610-2195

Jeffery F. Friedman

Department of Physics, University of Puerto Rico, Mayaguez, Puerto Rico 00681-9016 and Air Force Research Laboratory, Directed Energy Directorate, Kirtland Air Force Base, Albuquerque, New Mexico 87117-5776

Thomas M. Miller and A. A. Viggiano^{a)}

Air Force Research Laboratory, Space Vehicles Directorate, Hanscom Air Force Base, Bedford, Massachusetts 01731-3010

S. Denifl, P. Scheier, and T. D. Märk

Institut für Ionenphysik, Leopold-Franzen Universität, Technikerstrasse 25, A-6020 Innsbruck, Austria

J. Troe

Institut für Physikalische Chemie der Universität Göttingen, Tammannstrasse 6, D-37077 Göttingen, Germany

(Received 23 December 2005; accepted 23 January 2006; published online 31 March 2006)

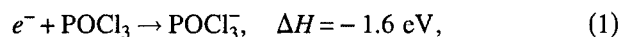
Two experimental techniques, electron swarm and electron beam, have been applied to the problem of electron attachment to POCl_3 , with results indicating that there is a competition between dissociation of the resonant POCl_3^* state and collisional stabilization of the parent anion. In the electron beam experiment at zero electron energy, the fragment ion POCl_2^- is the dominant ion product of attachment (96%), under single-collision conditions. Small amounts ($\sim 2\%$ each) of POCl_3^- and Cl^- were observed. POCl_3^- and POCl_2^- ion products were observed only at zero electron energy, but higher-energy resonances were recorded for POCl^- , Cl^- , and Cl_2^- ion products. In the electron swarm experiment, which was carried out in 0.4–7 Torr of He buffer gas, the parent anion branching ratio increased significantly with pressure and decreased with temperature. The electron attachment rate constant at 297 K was measured to be $(2.5 \pm 0.6) \times 10^{-7} \text{ cm}^3 \text{ s}^{-1}$, with ion products POCl_2^- (71%) and POCl_3^- (29%) in 1 Torr of He gas. The rate constant decreased as the electron temperature was increased above 1500 K. Theory is developed for (a) the unimolecular dissociation of the nascent POCl_3^* and (b) a stepladder collisional stabilization mechanism using the average energy transferred per collision as a parameter. These ideas were then used to model the experimental data. The modeling showed that $D_0^0(\text{Cl}-\text{POCl}_2)$ and $\text{EA}(\text{POCl}_3)$ must be the same within $\pm 0.03 \text{ eV}$. © 2006 American Institute of Physics. [DOI: 10.1063/1.2176613]

I. INTRODUCTION

A number of molecules attach low-energy electrons to form both the parent ion and a dissociative product. SF_6 is the most well studied of this class of molecules due to its importance as an electron scavenger in electrical devices.¹ Electron attachment to SF_6 is rapid and produces mainly SF_6^- at low temperatures and energies, but a slightly endothermic SF_5^- channel increases with electron energy and gas temperature. The predominance of SF_6^- production occurs even at low pressure, indicating that a very long-lived excited SF_6^* species exists.

Phosphoryl chloride (POCl_3) likewise attaches electrons rapidly, with dissociative and nondissociative channels, and

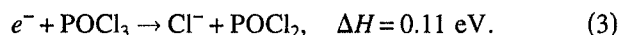
has been the subject of several recent studies.^{2–4} Zero-energy electron attachment forms two main ionic species; the parent anion,



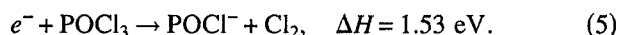
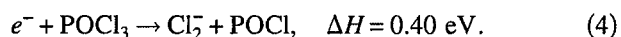
and POCl_2^- from a nearly thermoneutral channel



A third channel is observed in very low abundance



Two other channels are more endothermic:



The reaction enthalpies (at 298 K) given in Eqs. (1)–(5) are

^{a)}Author to whom correspondence should be addressed. Electronic mail: albert.viggiano@hanscom.af.mil

from GAUSSIAN 03 calculations⁵ reported in Ref. 4 and should be reliable within ± 0.1 eV. Electron attachment has been found to be almost as efficient as that of SF₆ with little variation in the total rate constant with temperature.² In contrast, the ratio of the product ions was found to be very dependent on temperature; increasing temperature decreased the amount of parent ion substantially in flowing-afterglow Langmuir probe (FALP) experiments performed at 1 Torr.² Increasing pressure leads to a substantial increase in the amount of parent, so that POCl₃⁻ is the dominant product at pressures greater than 100 Torr, even at elevated temperatures.³

Here we examine several further aspects of the attachment to POCl₃. The FALP apparatus at the Air Force Research Laboratory (AFRL) has recently been upgraded to allow for measurements as a function of electron temperature. Measurements of rate constants were performed as a function of electron temperature at four buffer gas temperatures. The technique is essentially a clone of that pioneered by Smith and Španěl.⁶ The results allow the different effects of internal and kinetic energy to be examined in the same experiment, much as is done for ion-molecule reactions.⁷ (See Christophorou and Olthoff for descriptions of electron swarm experiments, from which similar data may be obtained.¹) The temperature dependence of the branching ratios was reported earlier over the temperature range of 296–552 K at 1 Torr in He gas,² and the pressure dependence from 1 to 675 Torr in a N₂ buffer gas, at various temperatures.³ Here, we extend the measurements made in a helium buffer to cover a pressure range from 0.4 to 7 Torr at the same temperatures as earlier, and we have examined the dependence of the electron attachment rate constant on electron temperature. Further, an electron beam experiment was performed at the Leopold-Franzens University to determine branching ratios at essentially zero pressure. The latter experiment also includes an examination of higher-energy resonances, yielding dissociative products. On the theoretical side of the problem, we have analyzed the competition between the two main channels for both the new and earlier data using unimolecular rate theory.^{8–11} The results of this analysis may be applied to other situations in which the POCl₃⁻ undergoes thermal decomposition. The modeling also places a narrow limit on the difference between the electron affinity (EA) of POCl₃ and the bond dissociation energy of POCl₃⁻ (into POCl₂⁻ + Cl).

II. EXPERIMENT

A. AFRL FALP apparatus

The AFRL FALP apparatus has been described in detail previously and here only details important to the present results are given.¹² The FALP consists of a laminar, flowing electron-ion plasma created by an upstream microwave discharge in He (~ 1 Torr). For measurements in which the electrons are equilibrated with the buffer gas, that is, the electron temperature T_e is equal to the gas temperature T_g , a small amount of Ar ($\sim 2\%$) is added to the afterglow to eliminate He metastable states and He₂⁺. The electron density is measured along the length of the flow tube with a movable,

cylindrical Langmuir probe. The plasma velocity is measured by applying a small pulse to the microwave discharge and timing the propagation of the pulse along the flow tube axis with the Langmuir probe. In the electron-He⁺-Ar⁺ plasma, the electron density decays with distance due to ambipolar diffusion.

In the present work, POCl₃ gas¹³ was added (0.2–2 ppmV) to the plasma at a point downstream of the discharge after the plasma was thermalized, which resulted in a faster decay in the electron density along the flow tube axis downstream of the inlet. Eventually, all electrons had either undergone attachment or diffused to the walls of the flow tube.¹⁴ The data were fitted to solutions of the one-dimensional rate equations containing the diffusion and electron attachment loss rates. The fits, with and without the attaching gas present, yielded the electron attachment rate constant k_a and the ambipolar diffusion coefficient D_a . A quadrupole mass spectrometer at the terminus of the flow tube was used to identify the ion products formed and (at low mass resolution) to determine branching ratios. Relative peak heights were monitored as a function of neutral reactant concentration in order to distinguish primary from secondary product ions.

Pressure dependences in the thermal branching ratios were determined using the above procedure. Rate constant measurements were made only at pressures from 0.8 to 1 Torr, where D_a is small enough as to keep the determination of k_a reasonably accurate ($\pm 25\%$), and where electron-He collisions in the plasma sheath around the Langmuir probe are sparse enough as to not violate significantly the Mott-Langmuir criteria for the probe operation. The branching ratios were measured using very low concentrations of POCl₃ so that secondary ion chemistry is unimportant. Since the mass spectra are unrelated to the operation of the Langmuir probe, they can be obtained over a larger pressure range than can electron attachment rate constants.

While He quenches electron energy rapidly, Ar does not, because of the Ramsauer-Townsend minimum in the electron-Ar scattering cross section at thermal energies. Therefore, changing the buffer gas to Ar allows the study of electron attachment at T_e values of thousands of Kelvin. T_e may be varied by changing the fraction of the Ar buffer flowing through the microwave discharge and by adding some He to the afterglow. Measuring the electron temperature is accomplished by taking the second derivative of the current-voltage characteristic of the Langmuir probe, in the electron retarding region, as described by Španěl.¹⁵ Figure 1 shows the second derivative of the Langmuir probe current-voltage characteristic in the electron retarding region for different T_e . Electronic noise, the importance of patch fields on the surface of the probe, and the variation of T_e with distance along the flow tube result in an estimated 20% uncertainty in T_e in our experiment.

B. Innsbruck electron monochromator

High-resolution electron attachment to POCl₃ was studied at the Leopold-Franzens University, utilizing a hemispherical electron monochromator in conjunction with a

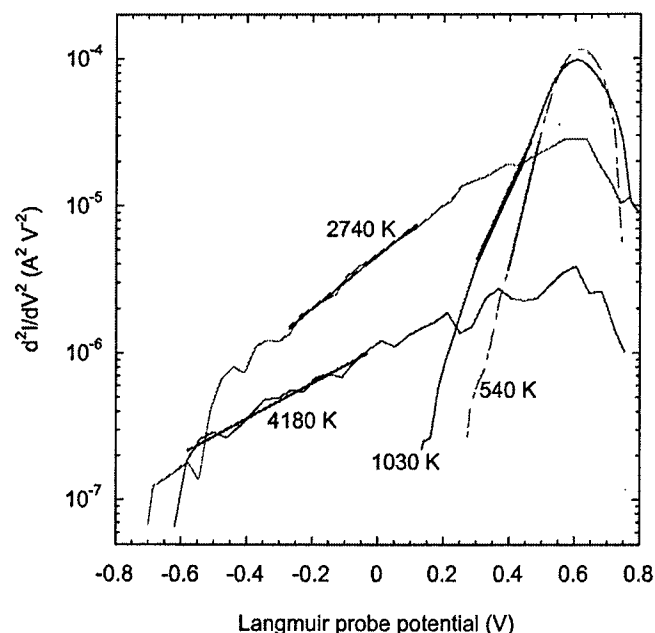
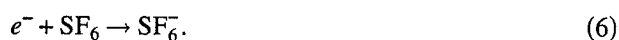


FIG. 1. Examples of fits to the second derivative of the Langmuir probe current-voltage characteristic in the electron retarding region to determine the electron temperature T_e . The thick lines show the fitted region. The curves have been moved laterally for clarity.

quadrupole mass spectrometer. A more detailed description can be found elsewhere.^{16,17} The electrons were produced by a heated filament and were accelerated with a lens system into a hemispherical electrostatic field analyzer, where the electron energy resolution was set for the present measurements to a value of 60–80 meV. In the past, we achieved at best an electron energy resolution of 35 meV with this monochromator.¹⁸ The present settings were a compromise between signal intensity and electron energy resolution. Following the hemispheres, the electrons were accelerated with a second lens system to the desired energy and focused into the collision chamber, where the electron beam intersected an effusive beam of POCl₃ at right angles.¹³ Anions formed in the collisions were extracted by a weak electric field (at maximum 200 meV/cm) and were mass analyzed with a high-resolution quadrupole mass spectrometer (maximum mass range of 2048 amu). The ion current was amplified by a channeltron-type secondary electron multiplier operated in a pulse counting mode and was recorded by a computer. The temperature of the gas beam was about 330 K. The residual gas pressure in the main chamber was 6.8×10^{-8} Torr. During the electron attachment measurements the pressure in the chamber was 1.3×10^{-7} Torr, measured with an ionization gauge.

The electron energy scale was determined by measuring the ion yield of a calibration gas under identical conditions. The following attachment reaction was used for calibration:



The ion yield of SF₆⁻ formed via reaction (6) exhibits a sharp peak at about 0 eV formed via *s*-wave attachment to the corresponding neutral molecules.¹⁹ The electron energy resolution was determined as the full width at half maximum of

TABLE I. Rate constants ($\pm 25\%$) and branching ratios ($\pm 5\%$ points) for electron attachment to POCl₃ using the FALP apparatus in 1 Torr He gas. The small Cl⁻ ion signal ($\sim 1\%$) is not included (see text).

T (K)	Rate constant (cm ³ s ⁻¹)	POCl ₃ fraction	POCl ₂ fraction
297	2.5×10^{-7}	29%	71%
372	2.2×10^{-7}	20%	80%
457	2.2×10^{-7}	6%	94%
552	2.0×10^{-7}	2%	98%

the nominal 0 eV peak. The ion residence time during extraction is estimated at 100–200 μs .

III. EXPERIMENTAL RESULTS

A. Electron attachment rate constants

Both the FALP and electron beam experiments show that POCl₃ attaches electrons efficiently for near zero-energy electrons. Electron attachment rate constants k_a were measured with the FALP apparatus in 1 Torr He gas, for temperatures of 300–552 K, under conditions where $T_e = T_g$, and are listed in Table I along with ion product branching ratios. For reasons given below, the small Cl⁻ ion product ($\sim 1\%$) was not included. The measured k_a are, on average, 25% greater than those reported in our 1998 paper, which were estimated accurate to within $\pm 25\%$. It is not possible to pinpoint the source of the difference except to say that it is difficult to measure fast electron attachment rate constants with the FALP apparatus: to satisfy first-order kinetics requirements, the concentration of reactant must exceed the initial electron density by a factor of 10. The lowest initial electron density (at the reactant port) that is feasible in FALP experiments (for clear Langmuir probe signal) is about 10^9 cm⁻³, so that the minimum reactant concentration is about 10^{10} cm⁻³. Though relatively small (300 ppbv), cou-

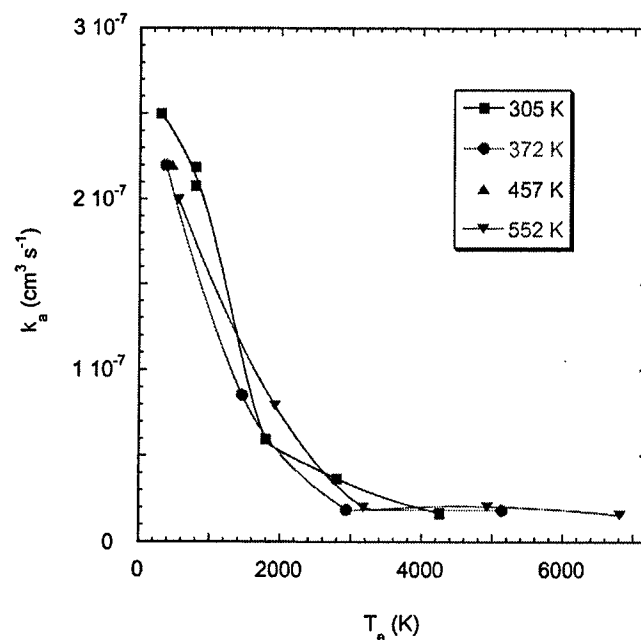


FIG. 2. Rate constants for electron attachment to POCl₃ measured for various T_e and T_g in the FALP experiment.

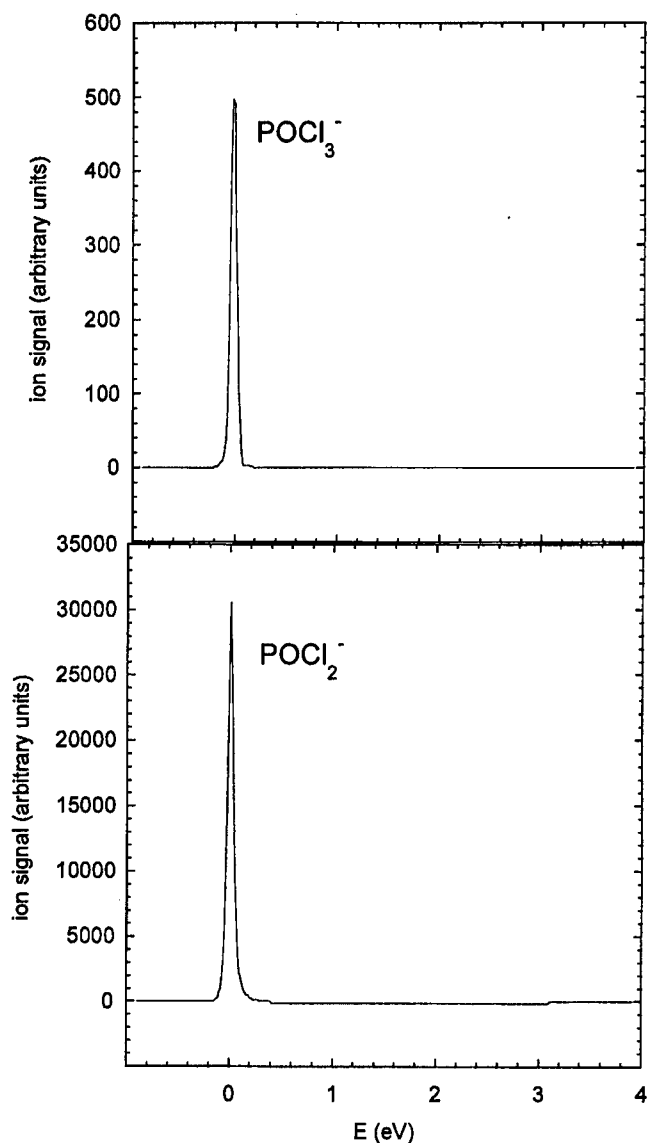


FIG. 3. Resonances observed in electron attachment to POCl_3 with the electron monochromator experiment, leading to POCl_3^- and POCl_2^- ion products.

pling this with the large attachment rate constant means that the reaction goes to completion over a distance of only 5 cm along the flow tube axis.

The FALP was also operated with Ar gas, which allowed measurements to be made at high T_e at different T_g . The k_a are plotted in Fig. 2 and are seen to rapidly decrease with increasing T_e . The k_a obtained at elevated T_e are more difficult to measure because the electron densities tend to be lower in the Ar afterglow. The k_a at high T_e shown in Fig. 2 are estimated accurate to $\pm 50\%$, and the electron temperature is estimated accurate to $\pm 20\%$. Within these uncertainties, data taken at different gas temperatures are similar.

B. Higher-energy resonances

Electron attachment resonances were observed in the monochromator experiment for POCl_3^- , POCl_2^- , POCl^- , Cl^- , and Cl_2^- ion products, as shown in Figs. 3 and 4. The first two channels were active only for near zero-energy electrons. The POCl^- product appeared only in a resonance centered at

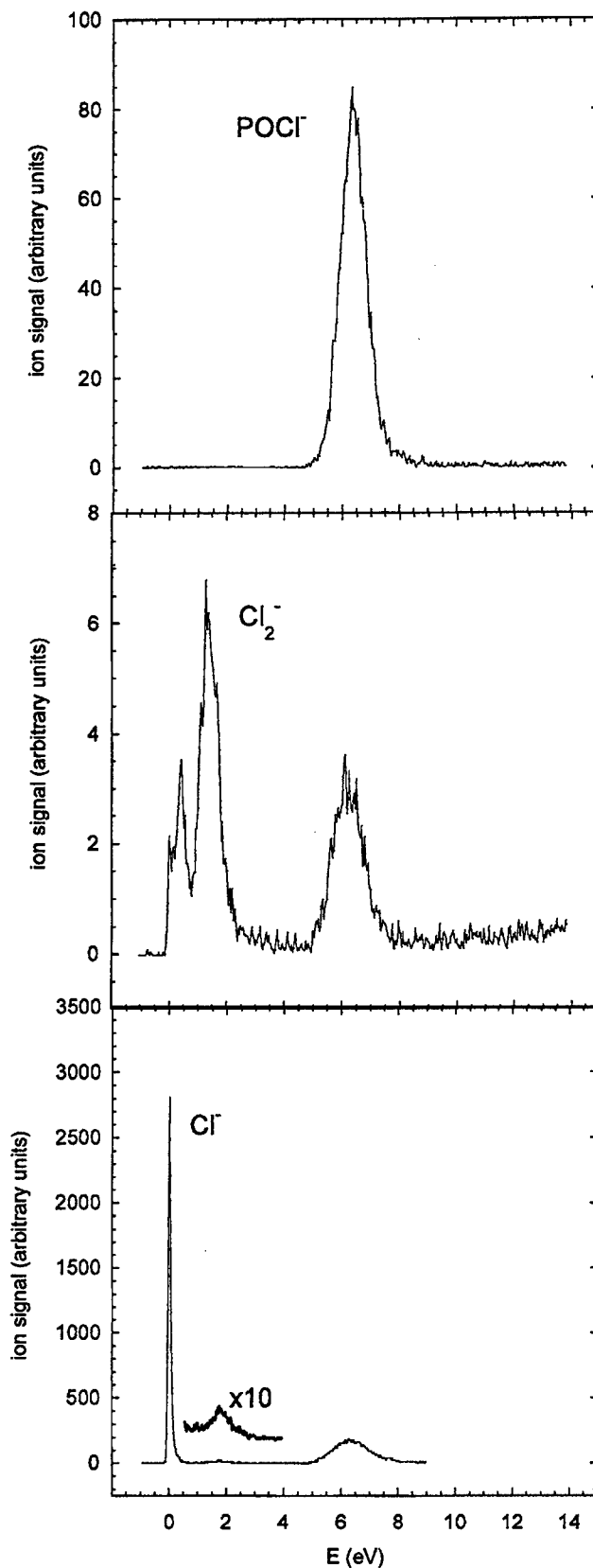


FIG. 4. Resonances observed in electron attachment to POCl_3 , leading to POCl^- , Cl_2^- , and Cl^- ion products.

6.4 eV. The Cl^- product was observed most strongly near zero electron energy, followed by a very weak resonance at 1.8 eV, and a modest one at 6.3 eV. The very weak Cl_2^- channel shows resonances at 0.5, 1.4, and 6.2 eV. The reso-

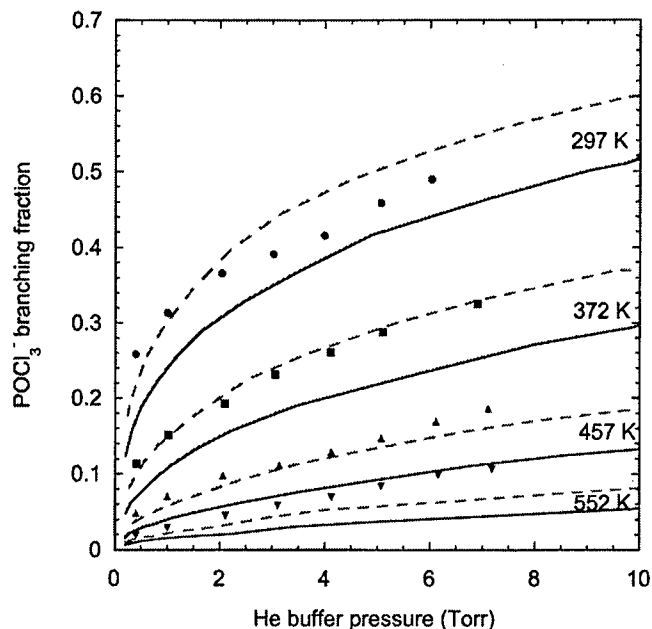


FIG. 5. Experimental (symbols) and modeled (curves) branching ratios $[\text{POCl}_2^-]/([\text{POCl}_3^-] + [\text{POCl}_2^-]) = S/(S+D)$ in the buffer gas He. Modeling parameters: $-\langle\Delta E\rangle/hc = 180 \text{ cm}^{-1}$ (dashed curves) and 90 cm^{-1} (solid curves); $f_{\text{rigid}} = 0.15$.

nance at 0.5 eV is close to the calculated endothermicity for the production of Cl_2^- , as given in Eq. (4). The close vicinity of the resonances at 6.4, 6.3, and 6.2 eV for the three product ions POCl_2^- , Cl^- , and Cl_2^- , respectively, indicates that a common transitory negative ion (TNI) subsequently dissociates into these competing channels. The excess energy between the position of these resonances and the thermochemical thresholds given in Eqs. (3)–(5) is distributed between the kinetic energy of the fragments and excitation energy of internal degrees of freedom of the molecular fragments.

C. Stabilization of the parent anion

At very low pressures, where no collisions occur before ions are detected, the electron beam experiment showed ion products POCl_2^- , Cl^- , and POCl_3^- , with relative intensities $\text{POCl}_2^-/\text{Cl}^-/\text{POCl}_3^-$ of about 47:1.2:1. That is, about 2% of the parent anions formed in the collisions survives to the detector, implying that a few of the nascent parent anions have either a lifetime longer than the 100–200 μs flight time or undergo stabilization (via radiative or internal vibrational relaxation). In the FALP experiment with helium buffer pressures in the range of 0.4–7 Torr, significant stabilization of the parent anion was observed upon electron attachment.² The POCl_3^- branching ratio reached 49% at 6 Torr at room temperature. A lower branching ratio was measured at elevated temperatures (e.g., 10% at this same pressure at 552 K). Earlier room temperature experiments in a nitrogen buffer had shown a branching ratio of 90% at 675 Torr.³ These results are qualitatively explained by resonant capture of an electron into a continuum state of POCl_3^- , which then undergoes either autodetachment, collisional stabilization, or decomposition. The yields of the parent anion in He and N_2 buffer gases are shown in Figs. 5 and 6, along with modeling results, of which more shall be said later.

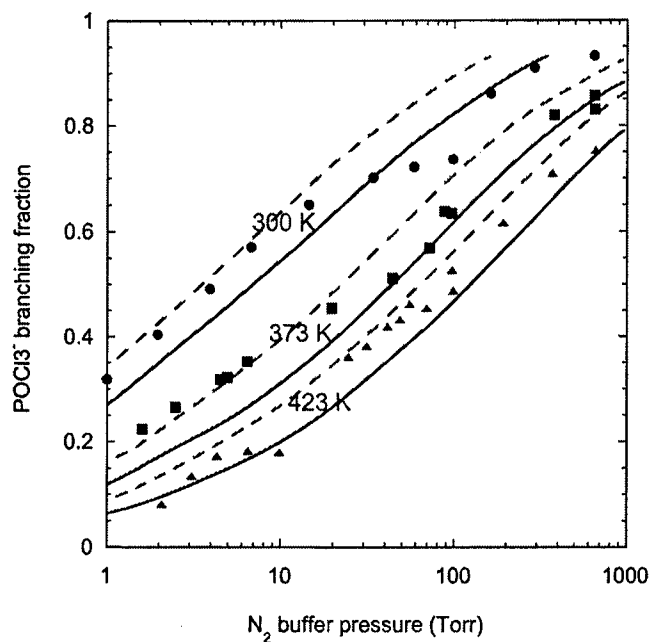


FIG. 6. As labeled in Fig. 5, for the buffer gas N_2 , with experimental data from Ref. 3. Modeling parameters: $-\langle\Delta E\rangle/hc = 125 \text{ cm}^{-1}$; $f_{\text{rigid}} = 0.1$ (dashed curves) and 0.2 (solid curves).

D. Yield of fragment anions

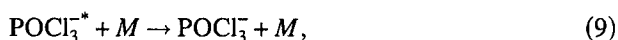
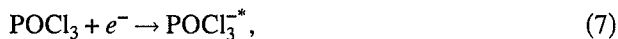
Let us first address the issue of the low abundance of Cl^- ions observed in both experiments. Calculations show this channel, Eq. (3), to be 0.11 eV endothermic at 298 K, though the calculations carry an uncertainty of that same order.⁴ In an earlier AFRL publication on this topic, Cl^- was said to be a direct product of attachment to POCl_3 because the branching ratio increased from 0.6% to 5% over the temperature range of 296–552 K.² In the present work with the FALP apparatus, with the helium buffer gas pressure varied between 0.4 and 7 Torr and temperature varied between 298 and 552 K, the Cl^- ion intensity remained in the neighborhood of 1% of the total ion intensity and did not vary in any systematic manner with pressure and temperature. Thus, the present conclusion from the FALP work is that the Cl^- may be a result of impurities, possibly introduced from prior work with chlorine compounds. An experiment carried out at Montana State University in a N_2 buffer gas from 1 to 675 Torr found that the Cl^- ion intensity never exceeds 1% of the total ion signal.³ However, in the electron beam experiments under single-collision conditions, Cl^- was observed at $\sim 2\%$, and the latter ratio was independent of pressure variations of POCl_3 in the main chamber from 1.3 to 6×10^{-7} Torr. The positions of Cl^- resonances at higher electron energy were also independent of the gas pressure. The conclusion from these and other tests with the Innsbruck electron monochromator on cation appearance energies is that the Cl^- is a direct product of attachment to POCl_3 . Whether this difference between the two experiments is real and related to collisional effects or due to impurities remains unresolved. It is obviously difficult to draw definite conclusions about very small ion products, especially when the neutral is reactive.

Under single-collision conditions, the major ion product of attachment is POCl_2^- observed in the Innsbruck work with

a branching ratio of 96%. The favoring of the POCl_2^- channel [Eq. (2)] over the Cl^- channel [Eq. (3)] is in harmony with calculations which give $\text{EA}(\text{POCl}_2)$ slightly greater than the known $\text{EA}(\text{Cl})$, and consequently, $D_{298}^0(\text{Cl}-\text{POCl}_2^-)$ is predicted to be smaller than $D_{298}^0(\text{POCl}_2-\text{Cl}^-)$ by 0.1 eV.⁴ Note that these channels differ only in the location of the electron. Often in dissociative recombination, these are attributed to differences in the potential energy surface near the attachment region. However, the presence of the parent anion reveals that the dynamics are mainly controlled by unimolecular decomposition and not the initial attachment step. In the present FALP experiments in a He buffer, and in earlier work in a N_2 buffer, smaller yields of POCl_2^- were observed, due to collisional stabilization of the parent anion. The present POCl_2^- branching ratios are given in Table I for 1 Torr of He gas. At other He pressures the POCl_2^- branching ratios may be deduced from the data in Fig. 5, since POCl_3^- is the only other ion product in the FALP work (aside from the ambiguous Cl^- product).

IV. THEORETICAL TREATMENT

The origin of the pressure dependence of the branching between POCl_3^- and POCl_2^- was attributed to the mechanism²⁻⁴



where the dissociation step (8) involves a long-lived vibrationally excited POCl_3^* species. The present analysis provides a quantitative investigation of this hypothesis. Denoting $[\text{POCl}_3^-]$ by S (stabilization), $[\text{POCl}_2^-]$ by D (dissociation), the rate coefficient of process (8) by k_{diss} , and the pseudo-first-order rate coefficient of the collisional stabilization step (9) by $k_{\text{stab}}[M]$, the branching ratio $S/(S+D)$ for POCl_3^- formation is symbolically written as

$$\frac{S}{S+D} = \frac{k_{\text{stab}}[M]}{k_{\text{stab}}[M] + k_{\text{diss}}} = \frac{1}{1 + k_{\text{diss}}/k_{\text{stab}}[M]} \quad (10)$$

In the most rigorous treatment, $S/(S+D)$ would have to be determined by the solution of a two-dimensional master equation in the space of the rovibrational energy E and the total angular momentum (quantum number J) of the species POCl_3^* . In this treatment k_{diss} would have to be replaced by the specific rate constants $k(E, J)$ for unimolecular dissociation of POCl_3^* and k_{stab} by the collisional stabilization rate coefficients $\gamma_c Z$, where Z denotes the total rate constant for energy transfer and γ_c is a collision efficiency resulting from the solution of the master equation for multistep rovibrational energy transfer. We do not have the required detailed information on $k(E, J)$ and on the state-to-state collisional energy- and angular momentum-transfer rates, determining γ_c . Therefore, in the following a simplified treatment is proposed which goes beyond that given in Ref. 3 and resolves some of the observed inconsistencies.

Equation (10) indicates that $S/(S+D)$ depends on the ratio of $k_{\text{diss}}/k_{\text{stab}}[M]$. A comparison of modeled and experimental $S/(S+D)$ thus can lead to only a single fit parameter which, to a first approximation, is given by the ratio of one fit parameter in k_{diss} and one in k_{stab} . (As a consequence of the multistep character of the system the fit parameter is only approximately given by the ratio, see below.) In our model, we derive the fit parameters from the measured $S/(S+D)$. The results then are analyzed and compared with energy transfer and dissociation rates from related reaction systems.

A. Specific rate constants for dissociation

Because of the lack of more detailed information on the transition state associated with the dissociation process (8), k_{diss} in Ref. 3 was estimated by simple Rice-Ramsperger-Kassel (RRK) theory in the form $k_{\text{diss}} \approx \nu[(E-E_0)/E]^s$, where ν is "the frequency of the active oscillator," s is the number of vibrational degrees of freedom, and E_0 is the dissociation threshold energy. In the present work we adopt a different point of view. As the process (8) is assumed to correspond to a simple bond fission reaction without a reverse barrier, it appears more appropriate to start with $k(E, J)$ from phase space theory (PST) such as relevant for an isotropic potential energy surface for process (8). The anisotropy then is accounted for by a rigidity factor f_{rigid} [see the statistical adiabatic channel model/classical trajectory (SACM/CT) approach of Refs. 8–11]. We therefore express $k(E, J)$ by

$$k(E, J) = f_{\text{rigid}}(E, J)k(E, J)^{\text{PST}} \quad (11)$$

Due to the lack of information on the potential, we simplify Eq. (11) by assuming that there is only a small J dependence of $k(E, J)$ (see, for instance, Refs. 9–11). In a first approximation, we further assume that $f_{\text{rigid}}(E, J)$ is a constant fit parameter over the relevant energy range. This assumption is later called into question. We therefore estimate k_{diss} to be of the form

$$k_{\text{diss}} \approx k(E, J=0) \approx f_{\text{rigid}}k(E, J=0)^{\text{PST}}, \quad (12)$$

where $k(E, J=0)^{\text{PST}}$ is obtained by convoluting the number of "open channels" (or "activated complex states") $W(E, J=0)^{\text{PST}}$ for the transitional modes of an atom+spherical top system²⁰ with the contributions from the conserved modes of POCl_2^- (see Table II). We employ a state counting algorithm such as described in the Appendix of Ref. 21.

In order to start the fitting procedure, a semiquantitative estimate of f_{rigid} has to be made. The dissociation process (8) at long range leads into a comparably weak ion-induced dipole potential which is isotropic and corresponds to $f_{\text{rigid}}=1$. It is known that ion-molecule potentials of this type at short range are governed by valence-type potentials (see, for instance, Refs. 22–24) which correspond to values of f_{rigid} smaller than unity. We have analyzed valence potentials from *ab initio* calculations for neutral molecules such as HO_2 , NO_2 , and H_2O_2 (see Refs. 25–27) and found that $f_{\text{rigid}}(E, J=0)$ was of the order of 0.1–1 and showed only a weak energy dependence. On the other hand, modeled short-range valence/long-range ion-induced dipole switching potentials

TABLE II. Molecular parameters used in the modeling.

Molecule and point group	Frequencies ^a (cm ⁻¹)	Product of rotational constants ^a
POCl ₃ (C _{3v})	1318.9, 567.4, 567.4, 461.4, 325.7, 325.7, 258.9, 183.1, 183.1	ABC=2.15 × 10 ⁻⁴ cm ⁻³
POCl ₂ (C _v)	1245.8, 405.6, 387.5, 271.7, 210.5, 174.8, 131.1, 81.7, 40.1	
POCl ₂ (C _v)	1214.7, 396.7, 333.3, 253.6, 201.2, 128.6	ABC=8.04 × 10 ⁻⁴ cm ⁻³

Additional quantities:^b
 EA(POCl₃)=1.59 eV=hc12 790 cm⁻¹
 E₀(POCl₃⁻→POCl₂⁻+Cl)=hc12 905 cm⁻¹
 α(He)=0.205 Å³
 α(N₂)=1.740 Å³

^aFrequencies and rotational constants were obtained from unscaled B3LYP/6-311+G(3df) calculations.

^bEA and E₀ from G3 calculations in Ref. 4; polarizabilities from Ref. 33.

for the dissociations of the cations of ethyl-, *n*-propyl-, and *n*-butyl-benzene in Refs. 9–11 led to energy-dependent f_{rigid} consistent with experimental determinations of $k(E)$.⁸ In this case, f_{rigid} was shown to be of the form

$$f_{\text{rigid}}(E, J) \approx [1 + \{[E - E_0(J)]/E_{\text{sw}}\}^m]^n \quad (13)$$

[with the bond dissociation energy $E_0(J)$ and the parameters $E_{\text{sw}}/hc=140$ cm⁻¹, $m=2$, and $n=-2/3$ for C₈H₁₀⁺].¹⁰ In the absence of more detailed knowledge on the potential of the POCl₃⁻ system, we started with a constant f_{rigid} but then also tested an energy-dependent f_{rigid} of the form expressed in Eq. (13).

Figure 7 shows $k(E, J=0)$ (for $f_{\text{rigid}}=0.15$) together with thermal rovibrational energy distributions $f(E, T)$ of neutral POCl₃. Following Refs. 2–4, we assume that during electron attachment (7) the rovibrational energy of POCl₃ is transferred into POCl₃⁻ and is fully available for dissociation (8) [restrictions by centrifugal barriers $E_0(J)$ and additional contributions from the energy of the electron are neglected]. It should be noted that the rovibrational average thermal energy of POCl₃ is equal to $\langle E_{\text{th}}(T) \rangle / hc = 990, 1400, \text{ and } 1700$ cm⁻¹ for $T=300, 373, \text{ and } 423$ K such as indicated by arrows in Fig. 7.

B. Collisional energy transfer rates

The overall rate coefficients for collisional energy transfer between POCl₃⁻ and the buffer gas M are estimated to be given by the Langevin rate constants $k_L = 2\pi e \sqrt{\alpha/\mu}$, with the electronic charge e , the polarizability α of the buffer gases, and the reduced mass μ of the POCl₃⁻+ M pairs. This gives $k_L(\text{POCl}_3^- + \text{N}_2) = 6.4 \times 10^{-10}$ cm³ molecule⁻¹ s⁻¹ and $k_L(\text{POCl}_3^- + \text{He}) = 5.4 \times 10^{-10}$ cm³ molecule⁻¹ s⁻¹. Instead of continuous state-to-state collisional transition probabilities, we use a stepladder model with down steps only where the step size is given by the absolute value of the average total energy $|\langle \Delta E \rangle|$ transferred per collision. For highly excited alkyl benzene cations, we estimated $-\langle \Delta E \rangle / hc$ to be of the order of 200–300 cm⁻¹ for He and N₂, respectively.^{9,10} As $\langle \Delta E \rangle$ is generally proportional to E and the present energies

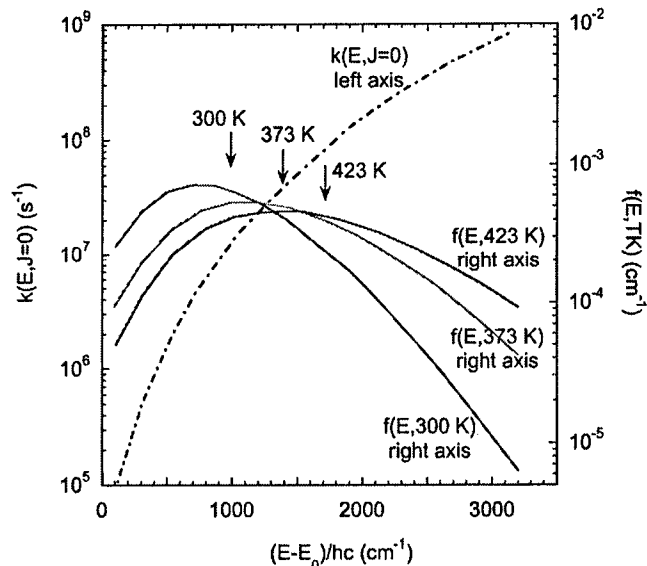


FIG. 7. Specific rate constants $k(E, J=0)$ (modeled with $f_{\text{rigid}}=0.15$) and thermal distributions $f(E, T)$ for the dissociation of POCl₃⁻ (at $T=300, 373, \text{ and } 423$ K from left to right at small E ; the arrows indicate average thermal energies $\langle E_{\text{th}} \rangle$ of POCl₃⁻ if $EA=E_0$).

are about one-half of those of the experiments with excited alkyl benzene cations,^{9,10} we estimate $-\langle \Delta E \rangle / hc$ to be of the order of 100–200 cm⁻¹. We repeat that one cannot expect to derive absolute values of $\langle \Delta E \rangle$ from the present measurements of $S/(S+D)$. Instead one will only be able to derive roughly the ratios of f_{rigid} and $\langle \Delta E \rangle$ [as long as the effective k_{diss} is proportional to f_{rigid} and k_{stab} is proportional to $\langle \Delta E \rangle$ in Eq. (10), see above].

C. Stepladder model for $S/(S+D)$

Chemical activation systems such as reactions (7)–(9) in the past often have been treated by stepladder models (see, e.g., Refs. 28–31) whenever more detailed information on collisional transition probabilities was lacking. Often solutions of master equations were also found to be equivalent to the results from stepladder models.³¹ Applying a stepladder model to the processes (7)–(9), we have

$$\left(\frac{S}{S+D} \right)_E = \prod_{i=1}^{T(E)} \frac{k_L[M]}{k_L[M] + k(E-i|\langle \Delta E \rangle)} \quad (14)$$

for a given initial energy E . $T(E)$ is equal to the number of steps between E and E_0 and is given by $(E-E_0)/|\langle \Delta E \rangle|$ (or more precisely by integer $[(E-E_0)/|\langle \Delta E \rangle| + 1]$). The value of $S/(S+D)$ needs to be thermally averaged over a thermal rovibrational energy distribution $f(E, T)$ of POCl₃. We note that the energy E in Eq. (12) corresponds to the total rovibrational energy of POCl₃⁻ and that the assumption of an only weak J dependence of $k(E, J)$ only applies when E is defined in this way. We, therefore, finally calculate

$$\frac{S}{S+D} = \int_0^\infty dE f(E, T) \prod_{i=1}^{T(E)} \{1 + k(E-i|\langle \Delta E \rangle)/k_L[M]\}^{-1}, \quad (15)$$

where $E=EA+E_{\text{th}}$ denotes the sum of the electron affinity (EA) of POCl₃ and its rovibrational thermal energy E_{th} (E

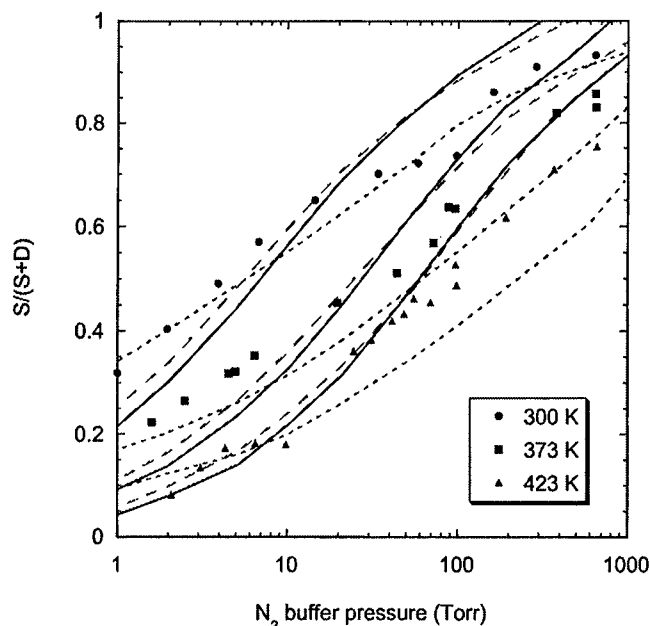


FIG. 8. As labeled in Fig. 5 with experimental points for N_2 buffer gas. Modeled curves are for energy dependent f_{rigid} given by Eq. (13) [full line, $E_0(J)=E_0(J=0)$, $E_{\text{sw}}/hc=280 \text{ cm}^{-1}$, $m=2$, $n=-2/3$, $-\langle\Delta E\rangle/hc=125 \text{ cm}^{-1}$], for energy-independent f_{rigid} with $EA=E_0+0.04 \text{ eV}$ (dashed line, $-\langle\Delta E\rangle/hc=500 \text{ cm}^{-1}$ $f_{\text{rigid}}=0.15$), and for energy-independent f_{rigid} with $EA=E_0-0.04 \text{ eV}$ (dotted line, $-\langle\Delta E\rangle/hc=62 \text{ cm}^{-1}$ and $f_{\text{rigid}}=1.0$).

$=0$ denotes the rovibrational zero point energy level of POCl_3 .

D. Modeling results

We started our modeling by assuming that E_0 is about equal to E_A (see Table II). Either varying $\langle\Delta E\rangle$, f_{rigid} was fitted or varying f_{rigid} , $\langle\Delta E\rangle$ was fitted such that the experimental $S/(S+D)$ curves as a function of the pressure P were reproduced. Figures 5 and 6 show the results for $M=N_2$ and He. One first observes that the experimental temperature and pressure dependences within the experimental scatter are well represented by our model with energy-independent f_{rigid} and temperature-independent $\langle\Delta E\rangle$. Figure 5 for the buffer gas $M=He$ shows slightly more scatter of the measurements around the modeled $S/(S+D)$ curves than Fig. 6 for $M=N_2$. Apparently this is due to the larger uncertainty of measuring small POCl_3 yields. We note again that we are unable to separate the fit parameters f_{rigid} and $\langle\Delta E\rangle$ because $S/(S+D)$ roughly depends only on the ratio $f_{\text{rigid}}/\langle\Delta E\rangle$. Nevertheless, the fit of $S/(S+D)$ over wide temperature and pressure ranges appears quite satisfactory and also allows for extrapolations outside the range of the present experiments.

In addition to the fit shown in Figs. 5 and 6 we have tested other possibilities. First, we have inspected the modeling of $S/(S+D)$ with energy-dependent rigidity factors such as given by Eq. (13), that means with rigidity factors which decrease with increasing energy. We observed that a consequence of this increase in all cases was a much steeper increase of $S/(S+D)$ with increasing pressure than was observed experimentally. Figure 8 shows one example with $E_{\text{sw}}/hc=280 \text{ cm}^{-1}$, $m=2$, $n=-2/3$ in Eq. (13), and $-\langle\Delta E\rangle/hc=125 \text{ cm}^{-1}$ for $M=N_2$. The experimental $S/(S$

$+D)$ thus clearly point towards a very weak energy dependence of f_{rigid} such as we observed for HO_2 , NO_2 , and H_2O_2 in contrast to the dissociations of cations of alkylbenzenes, see above.

Next we investigated the dependence of the modeled $S/(S+D)$ on the difference between the EA of POCl_3 and the dissociation energy E_0 of POCl_3 . Figure 8 includes modeled $S/(S+D)$ for one example with $EA=E_0+0.04 \text{ eV}$ (keeping $f_{\text{rigid}}=0.15$ and fitting $-\langle\Delta E\rangle/hc=500 \text{ cm}^{-1}$) and one example with $EA=E_0-0.04 \text{ eV}$ [choosing $f_{\text{rigid}}=1$ and fitting $-\langle\Delta E\rangle/hc=62 \text{ cm}^{-1}$ in order to reproduce $S/(S+D)$ at 300 K]. In all cases either the pressure or the temperature dependence of $S/(S+D)$ could not be well represented. $EA=E_0\pm 0.03 \text{ eV}$ was about the limit for which the observed $S/(S+D)$ could be fitted over the experimental range. We, therefore, conclude that

$$EA = E_0 \pm 0.03 \text{ eV} \quad (16)$$

is about the limit which is compatible with the experimental $S/(S+D)$. $EA=E_0\pm 0.1 \text{ eV}$ was determined in the G3 calculations of Ref. 4, in agreement with the present evaluations of $S/(S+D)$. If $EA=1.60\pm 0.1 \text{ eV}$ is taken from the G3 calculations of Ref. 4 (for 0 K), being in rough agreement with the experimental value of $EA=1.41 (+0.2/-0.1) \text{ eV}$ from Ref. 32, then the dissociation energy of POCl_3 in the process leading to POCl_2+Cl (for 0 K) from the present analysis of $S/(S+D)$ data follows as well as $E_0=1.60(\pm 0.1) \text{ eV}$.

We finally may rationalize our observation that about 2% of the parent ions at very low pressures have either dissociative lifetimes longer than 100–200 μs or undergo radiative stabilization. Inspecting Fig. 7, one sees that the low-energy tail of the thermal distribution reaches down to energies near E_0 , where $k(E, J=0)$ approaches a threshold value of $k(E=E_0, J=0)$ of about 100 s^{-1} . There is then indeed a fraction of the order of a percent of the thermal distribution which covers lifetimes in the range of 100 μs . However, this requires that EA is equal to $E_0\pm 0.01 \text{ eV}$, an even more stringent restriction than postulated by Eq. (16). One cannot rule out that there is also some radiative stabilization, but $EA=E_0\pm 0.01 \text{ eV}$ would be consistent with our observations.

A Cl^- yield in the percent range would also be compatible with a pathway via POCl_3 . If one shifts $k(E)$ by about 900 cm^{-1} to the right in Fig. 7, which corresponds to the energetics of Eq. (3), one has to expect Cl^- yields from reaction (3) in the percent range. However, our observations of the Cl^- yields are still far too scattered and incomplete to allow for more certain conclusions.

V. CONCLUSIONS

Experiments on the formation of ions in electron attachment to POCl_3 have been described along with a theoretical analysis of the results. The experimental results consist of (a) measurements of rate constants and product branching ratios for electron attachment to POCl_3 in a He buffer gas, under conditions where $T_e=T_g$ and $T_e>T_g$ (rate constants only); (b) determination of energies at which resonances occur in the attachment process for the various ion products POCl_3^- , POCl_2^- , POCl^- , Cl^- , and Cl_2^- ; and (c) branching ratios for the

ion products from single-collision conditions up to 7 Torr of He gas. These final data may be compared with earlier data obtained at 1–675 Torr of N₂ gas.³ The theoretical analysis presented here treated (a) the unimolecular dissociation of the vibrationally excited POCl₃^{*} formed in the resonant electron attachment process with a rate constant $k(E, J)$ obtained from phase space theory and an anisotropic contribution represented by a rigidity factor f_{rigid} and (b) the stabilization of the parent anion in collisions with the buffer gas, in terms of a stepladder model using the Langevin rate constant coupled with an average total energy $\langle \Delta E \rangle$ transferred per collision. Modeling of the experimental data using these concepts is quite satisfactory, which means that the parameters determined for $k(E, J)$, f_{rigid} , and $\langle \Delta E \rangle$ may be used in other situations where unimolecular dissociation and/or stabilization of POCl₃^{*} may be encountered. Finally, the modeling of the data places a narrow limit of ± 0.03 eV on the difference between $D_0^0(\text{Cl}-\text{POCl}_2)$ and $\text{EA}(\text{Cl})$.

ACKNOWLEDGMENTS

One of the authors (J.M.V.D.) acknowledges support from the National Academy of Sciences Air Force Summer Faculty Fellowship Program and from the College of the Holy Cross. This work was supported by the U.S. Air Force Office of Scientific Research, the Air Force European Office for Aerospace Research (EOARD Grant No. FA 8655-03-1-3034), the Deutsche Forschungsgemeinschaft (SFB 357 "Molekulare Mechanismen Unimolekularer Prozesse"), the FWF and ÖNB (Wien, Austria), and the European Commission (Brussels, Belgium). Another author (T.M.M.) is under contract (FA8718-04-C0006) to the Institute for Scientific Research of Boston College.

¹L. G. Christophorou and J. K. Olthoff, *Fundamental Electron Interactions with Plasma Processing Gases* (Kluwer/Academic, New York, 2004).

²T. M. Miller, J. V. Seeley, W. B. Knighton, R. F. Meads, A. A. Viggiano, R. A. Morris, J. M. Van Doren, J. Gu, and H. F. Schaefer III, *J. Chem. Phys.* **109**, 578 (1998).

³D. H. Williamson, C. A. Mayhew, W. B. Knighton, and E. P. Grimsrud, *J. Chem. Phys.* **113**, 11035 (2000).

⁴W. B. Knighton, T. M. Miller, E. P. Grimsrud, and A. A. Viggiano, *J. Chem. Phys.* **120**, 211 (2004).

⁵L. A. Curtiss, P. C. Redfern, K. Raghavachari, V. Rassolov, and J. A.

Pople, *J. Chem. Phys.* **109**, 7764 (1998); L. A. Curtiss, P. C. Redfern, and K. Raghavachari, *ibid.* **123**, 124107 (2005).

⁶D. Smith and P. Španěl, *Adv. At., Mol., Opt. Phys.* **32**, 307 (1994).

⁷R. A. Morris and A. A. Viggiano, *J. Phys. Chem.* **98**, 3740 (1994).

⁸A. I. Maergoiz, E. E. Nikitin, J. Troe, and V. G. Ushakov, *J. Chem. Phys.* **117**, 4201 (2002).

⁹J. Troe, A. A. Viggiano, and S. Williams, *J. Phys. Chem. A* **108**, 1574 (2004).

¹⁰J. Troe, V. G. Ushakov, and A. A. Viggiano, *Z. Phys. Chem.* **219**, 699 (2005).

¹¹J. Troe, V. G. Ushakov, and A. A. Viggiano, *Z. Phys. Chem.* **219**, 715 (2005); *J. Phys. Chem. A* **110**, 1491 (2006).

¹²T. M. Miller, A. E. S. Miller, J. F. Paulson, and X. Liu, *J. Chem. Phys.* **100**, 8841 (1994).

¹³The POCl₃ used in both locations was obtained (separately) from Sigma-Aldrich and had a stated purity of 99%.

¹⁴D. Smith and P. Španěl, *Adv. At., Mol., Opt. Phys.* **32**, 307 (1994).

¹⁵P. Španěl, *Int. J. Mass Spectrom. Ion Process.* **149/150**, 299 (1995). We used software developed by Španěl in the present experiment to determine both the electron density and the electron temperature from the Langmuir probe I - V characteristic.

¹⁶G. Hanel, B. Gstr, S. Denifl, P. Scheier, M. Probst, B. Farizon, M. Farizon, E. Illenberger, and T. D. Märk, *Phys. Rev. Lett.* **90**, 188104 (2003).

¹⁷S. Denifl, S. Ptasinska, M. Cingel, S. Matejcek, P. Scheier, and T. D. Märk, *Chem. Phys. Lett.* **377**, 74 (2003).

¹⁸D. Muigg, G. Denifl, A. Stamatovic, and T. D. Märk, *Chem. Phys.* **239**, 409 (1998).

¹⁹L. G. Christophorou and J. K. Olthoff, *Int. J. Mass. Spectrom.* **205**, 27 (2001).

²⁰M. Olzmann and J. Troe, *Ber. Bunsenges. Phys. Chem.* **96**, 1327 (1992); J. Troe, *J. Chem. Phys.* **79**, 6017 (1983); W. J. Chesnavich and M. T. Bowers, in *Gas Phase Ion Chemistry*, edited by M. T. Bowers (Academic, New York, 1979), Vol. 1, p. 119.

²¹D. C. Astholz, J. Troe, and W. Wieters, *J. Chem. Phys.* **70**, 5107 (1979).

²²S. Klippenstein, *Int. J. Mass Spectrom. Ion Process.* **167/168**, 235 (1997).

²³W. Kutzelnigg, V. Staemmler, and K. Hoheisel, *Chem. Phys.* **1**, 27 (1973).

²⁴F. Muntean and P. B. Armentrout, *J. Phys. Chem. A* **107**, 7413 (2003).

²⁵L. B. Harding, J. Troe, and V. G. Ushakov, *Phys. Chem. Chem. Phys.* **2**, 631 (2000).

²⁶J. Troe and V. G. Ushakov, *Phys. Chem. Chem. Phys.* (submitted).

²⁷B. Abel, J. Troe, and V. G. Ushakov, *Z. Phys. Chem.* (submitted).

²⁸G. H. Kohlmaier and B. S. Rabinovitch, *J. Chem. Phys.* **38**, 1709 (1963); **39**, 490 (1963).

²⁹D. W. Setser, B. S. Rabinovitch, and J. W. Simons, *J. Chem. Phys.* **40**, 1751 (1964).

³⁰W. Forst, *Theory of Unimolecular Reactions* (Academic, New York, 1973).

³¹J. Troe, *J. Phys. Chem.* **87**, 1800 (1983).

³²B. P. Mathur, E. W. Rothe, S. Y. Tang, and G. P. Pack, *J. Chem. Phys.* **65**, 565 (1976).

³³T. M. Miller, in *Handbook of Chemistry and Physics*, 86th ed., edited by D. R. Lide (CRC, Boca Raton, FL, 2005), Sec. 10, pp. 192–201.